IEEE Access
Multidisciplinary | Rapid Review | Open Access Journal

Received December 15, 2018, accepted December 27, 2018, date of publication January 8, 2019, date of current version January 23, 2019.

Digital Object Identifier 10.1109/ACCESS.2019.2891132

Kinematic Analysis of Trajectory Dimension-Dependent Sensorimotor Control in Arm Tracking

MENGYING FAN[1], JIE LUO[1], LE LI[2], DONG FENG HUANG[2,3], YINWEI ZHAN[4], AND RONG SONG[1]

[1]Key Laboratory of Sensing Technology and Biomedical Instrument of Guangdong Province, Guangdong Provincial Engineering and Technology Center of Advanced and Portable Medical Devices, School of Biomedical Engineering, Sun Yat-sen University, Guangzhou 510006, China
[2]Guangdong Engineering Technology Research Center for Rehabilitation Medicine and Clinical Translation, Department of Rehabilitation Medicine, The First Affliated Hospital, Sun Yat-sen University, Guangzhou 510080, China
[3]Xinhua College, Sun Yat-sen University, Guangzhou 510520, China
[4]School of Computer Science and Technology, Guangdong University of Technology, Guangzhou 510006, China

Corresponding author: Jie Luo (luoj26@mail.sysu.edu.cn)

This work was supported in part by the Guangdong Science and Technology Planning Project under Grant 2017A020211002, in part by the Project of Science and Technology Program of Guangdong Province under Grant 2017B010110015 and Grant 2017B010110007, in part by the Guangdong Science and Technology Planning Projects under Grant 2015B020214003 and Grant 2017B020210011, in part by the Natural Science Foundation of Guangdong Province under Grant 2015A030313139, and in part by the Sun Yat-sen University, China, through the 5010 Planning Project under Grant 2014001.

ABSTRACT This paper aims to examine how the trajectory dimension influences sensorimotor control during arm tracking. We designed three trajectories with different dimensions in a three-dimensional (3D) immersive virtual reality environment and instructed the subjects to control a virtual hand to follow a cubic target that moved along the designed trajectories. The position of the virtual hand was determined by the position of the actual hand captured with a high-resolution 3D motion capture system in real time. Five kinematic measures were calculated: the root mean square error (RMSE), the standard deviation of the speed ($speed_{sd}$), the magnitude of the jerk ($Jerk_m$), the integral of the speed power spectrum (IVPS), and the 3D fuzzy approximate entropy ($fApEn_{3D}$). All the kinematic measures increased significantly with increasing trajectory dimensions, except for the IVPS between the 1D and 2D conditions and the $fApEn_{3D}$ between the 2D and 3D conditions. The increase in time-domain parameters (i.e., RMSE, $speed_{sd}$, and $Jerk_m$) showed degradation in accuracy, energy efficiency, and multijoint coordination, respectively, in the higher dimensions. An increase in the frequency-domain measure (i.e., IVPS) in higher dimensional condition reflected an increase of visual feedback-related intermittency in manual control when increasing the trajectory dimension. The larger nonlinear $fApEn_{3D}$ values in the 2D and 3D conditions might have been due to the higher level neuromotor noise and increased sensory inputs. The selected parameters could provide a comprehensive method for evaluating motor performance from different perspectives. The findings in this paper shed light on the underlying sensorimotor control that is caused by the trajectory dimension in arm tracking tasks.

INDEX TERMS Neural engineering, kinematics, virtual reality, entropy, motion analysis.

I. INTRODUCTION

The sensorimotor control system of the human central nervous system (CNS) plays an important role in performing visually guided arm tracking, which is a widely used task for assessing the motor function of patients with neural-motor impairment [12], [32]. Previous experimental psychologists have proposed a three-stage model to account for the discrete response that the human CNS executes to a stimulus, and the three stages were: a continuous sensory analysis stage, a discrete response planning stage and a continuous response execution stage [22]. Based on the three-stage model, Neilson *et al.* [22] simulated tracking responses and illuminated that the closed-loop feedback control could adaptively stabilize the sensorimotor transform even if the

internal model was inaccurate, which pioneered the research on tracking responses to unveil the underlying sensorimotor mechanism. Instead of simulation, Miall *et al*. [20] measured the tracking responses, calculated the speed power spectra and proposed that the intermittency could be represented with a power element in the spectra and that the error-correction responses in tracking movements might be limited by a positional error deadzone. However, a more recent study based on arm tracking, instead of manual joystick tracking, showed that both speed and direction errors were involved in regulating the submovements, each of which corresponded to error-corrective response planning [27]. Moreover, Ao *et al*. [1] suggested that an integration of feedforward and feedback control contributed to arm tracking performance, and a shift from feedback to feedforward control was found in faster tracking movements. Patients after stroke tracked the target with less accuracy, which may be due to the increased neuromotor noise in the sensorimotor system [1]. Therefore, the external tracking performance should be capable of reflecting the internal regulation of sensorimotor control by the human CNS.

Many factors, such as target size [13], target speed [1], movement direction [11] and delayed visual feedback information [17], are all related to the underlying sensorimotor control during arm tracking. Huysmans *et al*. [13] manipulated the target size to change the precision level in a two-dimensional (2D) tracking task that was performed with a pen, and the results showed that increased precision demands were accommodated by both the different organization of submovements and increased muscle activity. Ao *et al*. [1] detected the effects of the target speed at 6 levels on feedforward-feedback control during elbow tracking tasks using sinusoidal trajectories, which indicated a shift from feedback to feedforward control as the target speed increased. Huang *et al*. [11] compared the tracking behaviors along four different directions during multijoint upper limb movements, and parametric differences in all four directions reflected notable influences on the movement direction in sensorimotor control. Limanowski *et al*. [17] changed the visual feedback delays of hand movements at eight lengths during sinusoidal tracking tasks at 0.5 Hz in three-dimensional (3D) space and tracked the accuracy and brain activity using functional magnetic resonance imaging (fMRI), which showed that a distributed network of brain regions was used to process visual information at different stages to accurately guide one's actions online.

The trajectory dimension, which is the minimum number of independent variables (or degrees of freedom (DOF)) that determines a curve [23], [24], can also influence sensorimotor control in arm tracking. For example, lines in a plane possess only one DOF, and the trajectory dimension of the straight lines should be 1, regardless of their angle in the plane. Circles or other trajectories in a plane with uncorrelated projection movements in a Cartesian coordinate frame should be 2D trajectories. Similarly, if the deviations in the x-, y- and z-coordinates (where x is the horizontal axis from left to right, y is the horizontal axis from posterior to anterior, and z is the vertical axis perpendicular to the horizontal plane) are not related to one another, then the trajectory dimension is considered to be 3. Watson and Jones [31] designed a 2D random-tracking trajectory as two orthogonal one-dimensional (1D) equivalents (i.e., x only and y only) and found a deterioration in tracking performance on 2D tasks compared with that on 1D tasks according to the error scores. The same observation was made by Oytam *et al*. [24], who suggested that horizontal performance was superior to 2D (or two simultaneous one-DOF movements) performance.

Kinematic outcome measures exhibit sensitivity and reliability in assessing sensorimotor control. Error signals have been used to investigate tracking performance when changing from a 1D to a 2D tracking task [24], [31]. Speed fluctuation, speed_{sd}, is a measure that quantifies the variations in instantaneous speed around the mean speed and often serves as an estimation of energy cost and movement efficiency [2]. Parameters relevant to jerk have been widely used to quantify the smoothness of the movement path and to reflect abnormal muscle tone [34]. Apart from these temporal characteristics, sensorimotor control can also be evaluated in terms of frequency characteristics. The power spectrum is a frequency parameter that is calculated from the speed signals, and the values of the power spectrum in the frequency band that range from 0.5 to 1.8 Hz during visual tracking are larger than those of nonvisual tracking movements [20]. A previous study suggested that the integral of the power spectrum of normalized speed values could reflect the shift between feedback and feedforward control [1]. The human motor system has the potential to adjust its behavior under the influence of organismic, task and environmental constraints, and these adaptability characteristics could be better measured by nonlinear entropy measurements. ApEn has been selected to estimate the effects of postural balance based on simulated random time-series data [14], [25]. fApEn is a generalized version of ApEn, showing better monotonicity, better relative consistency, and more robustness to noise when characterizing signals with different complexities. fApEn analysis has been employed to investigate stroke-induced changes in sensorimotor control [34] and steady-state visual evoked potentials-based preictal alert to migraine patients [4]. Moreover, fApEn could provide insight into discriminating the aging-related changes in the coordination of agonist and antagonist muscles [29]. fApEn is most likely capable of providing insight into the variability of sensory inputs [3] and neuromotor noise [19], [34].

Although many researchers have focused on the effect of the trajectory dimension, whether higher dimensions in tracking tasks are more demanding on the CNS remains unclear. Most previous researchers have used only error scores to investigate the influence of trajectory dimension on sensorimotor control. A kinematic analysis of dimension-dependent sensorimotor control using multiple measures is important but has not yet been performed. We designed three trajectories with different DOFs, and a head-mounted display (HMD) was

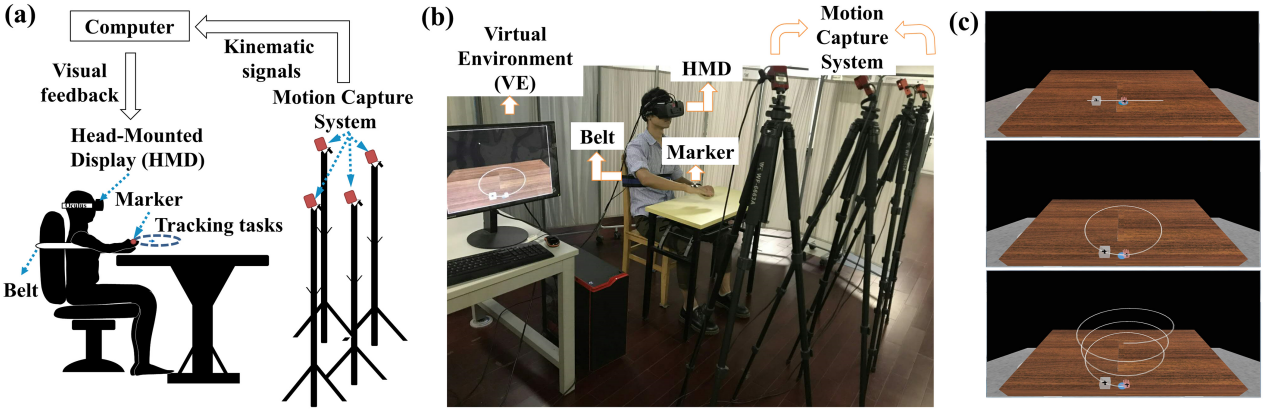

FIGURE 1. Experimental setup and tracking trajectories. (a) A schematic drawing of the experimental setup. (b) A picture of the real virtual reality system. (c) The virtual scenes of the tracking tasks: the target (a semitransparent cube with a cross in the center) moved along one of the three preset trajectories, including a horizontal line (one dimension, 1D), a circle (two dimension, 2D) and a cylindrical helix (three dimension, 3D). The subjects controlled the virtual hand (the pink palm with a cross in the center) to move in the same way as the target, which means that the two crosses in the target cube and the virtual hand should overlap with each other as well as possible. The blue circle on the table is the home position, i.e., the starting point of the movement for each trial, and the whole preset trajectory could be seen from the very beginning of the trial. The target was not tracked in (b) and (c), so the crosses in the virtual hand and the target cube could both be shown for the sake of clarity.

used to provide 3D visual feedback. Five kinematic measures characterized the time-domain (RMSE, $speed_{sd}$ and $Jerk_m$) and frequency-domain properties (IVPS); in addition, linear (RMSE, $speed_{sd}$, $Jerk_m$ and IVPS) and nonlinear dynamical features ($fApEn_{3D}$) were selected to provide comprehensive perspectives on the sensorimotor control of arm tracking movements.

II. MATERIAL AND METHODS

A. SUBJECTS

A total of 21 healthy right-handed adults (9 males and 12 females, mean age: 21.67 ± 1.91 years) were recruited for this study. The criteria for inclusion were (1) good visual acuity and mental capacity, such that wearing a HMD would not cause psychological or physical discomfort; (2) good understanding and tracking ability; and (3) capability of providing informed consent. Before the experiment, all the subjects were informed of the procedure and gave written informed consent for this study. Ethical approval was provided by the Medical Ethical Committee of the First Affiliated Hospital of Sun Yat-sen University.

B. APPARATUS

As shown in Fig. 1a, the subjects were seated on a comfortable chair with a HMD (Oculus version DK2, California, USA). Restraining seat belts were used to prevent trunk flexion during tracking. The experiment was conducted in a quiet room with the light off to avoid noise and interference. During the arm tracking tasks, kinematic data of the hand were captured using a marker-based motion capture system (OptiTrack, NaturalPoint, USA) at 100 frames per second; the marker was firmly fixed to the second metacarpals. The movement of a virtual hand in the HMD was driven by the recording of the actual hand's displacement in real time, and the 3D cubic target could move in its trajectory at a constant speed (tangential speed: 2.25 cm/s). According to [27], 2.25 cm/s is a slow target speed, which can provide subjects enough time to integrate the sensory information and minimize the influence of the transmission delay on generating motor commands to modulate their real time feedback control performance. As shown in Fig. 1c, there were three types of trajectories in the experiment: 1) a horizontal line, 2) a horizontal circle and 3) a vertical cylindrical helix. For these trajectories, the independent variables that determined the curve were 1, 2 and 3, respectively, and the trajectory's different coordinate projections were uncorrelated with one another. Therefore, the dimensions of these trajectories were 1, 2 and 3, respectively. The length of the horizontal line was 24 cm in the 1D condition. The radius of the horizontal circle was 12 cm in the 2D condition. In the 3D condition, the radius of the horizontal circle projected by the cylindrical helix was also 12 cm, and the height of the helical pitch was 6 cm. Therefore, the times required to finish single tracking loops for the 1D, 2D and 3D conditions were21.3 s, 33.5 s and 33.6 s, respectively. In the 3D condition, the overall vertical displacement was 18 cm. To generate a more realistic 3D view, the designed trajectory was visible to the subjects at the beginning of and during the whole tracking, but the actual trajectory drawn by the participants was not presented. The visibility of the trajectory might help the subjects with their predictive forward control in arm tracking, hence minimizing the time delay during tracking. The target was a semitransparent cube that was 3 × 3 × 3 cm in size, and the virtual hand was a scaled solid pink palm (reduced by approximately 70% in size compared to the general size of human hands, which was chosen during the pre-experiments based on subjects' satisfaction). In addition, black crosses were drawn in the center of the target and the virtual hand. When the two crosses overlapped with each other, the error was minimized. The blue solid circle (1-cm radius) on the virtual desk represented

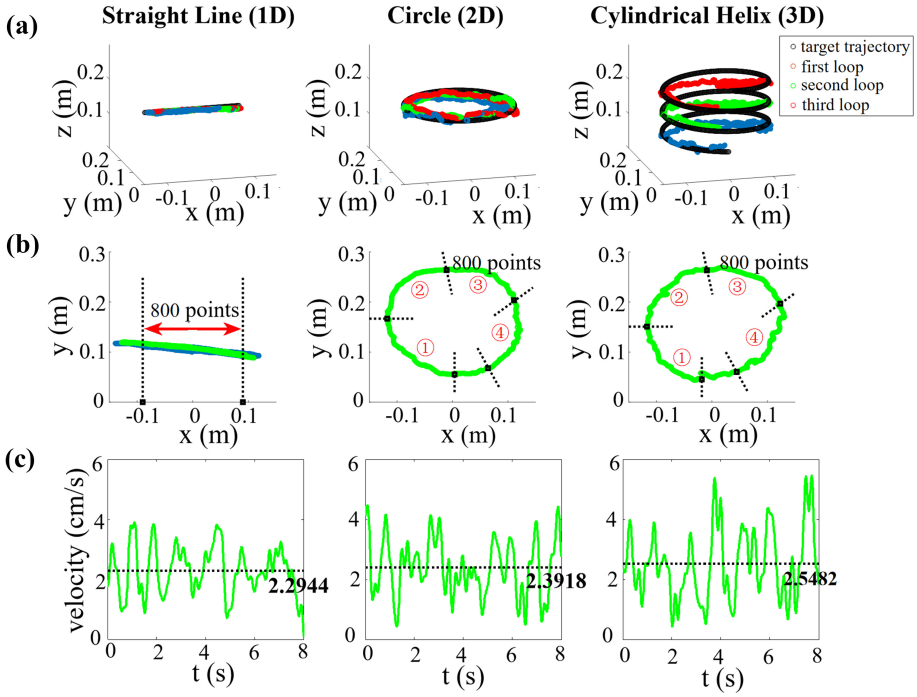

FIGURE 2. (a) The target (black) trajectories and a sample of the actual tracking trajectories performed in the 1D, 2D and 3D conditions. Here, x stands for the horizontal axis from left to right, y represents the horizontal axis from posterior to anterior, and z is the vertical axis perpendicular to the horizontal plan. The real tracking trajectories were segmented into the first loop (blue), second loop (green) and third loop (red) for the sake of clarity. (b) The data we selected for use in calculating the kinematic measures were obtained from the raw signals. To calculate all the kinematic measures, the data length was chosen as 800 for the 1D condition, corresponding to about the central 18 cm of the actual trajectory. To calculate all the kinematic measures except the IVPS, the second loop was selected for the 2D and 3D conditions. For comparison with the IVPS for the 1D condition, 4 consecutive 800-point segments were extracted from the second loop in the 2D and 3D conditions. (c) The speed pulses calculated from the 800-point extracted data in the 1D, 2D and 3D conditions. The horizontal dashed line represents the mean speed.

the home position of the movement. The subjects could put their hands on this circle when they had rest periods during the experiments, which occurred between each pair of successive trials. The virtual environment (VE) was generated using OpenGL in C++, and the virtual hand was modeled through 3ds Max. The field angles (FOV) of the HMD were set according to the vision range of the human eye (horizontal field angle: 120°; vertical field angle: 60°), providing an immersive virtual reality experience for the subjects.

C. EXPERIMENTAL PROCEDURES

1) TRIAL

A trial began with the participant's hand at the home position (blue circle) on the virtual desk. Once the hand was lifted to a height of approximately 8 cm above the table and paused for 2 s, a virtual target appeared in the HMD and began to move. In the 1D condition, the target started moving from the center to the left and then to the right and back to the center. While tracking the target along the horizontal line, the hand followed the target back and forth three times continuously. In the 2D and 3D conditions, the subjects were required to track the target along the circle three times and along the cylindrical helix once as a trial in the clockwise direction, and the movement started at the point closest to the body. During tracking, the subjects were required to follow the moving target as closely as possible. An exact overlap of the two crosses represented perfect tracking accuracy. There was a 2-min rest between each pair of successive trials.

2) TRAINING BLOCK

The participants who were recruited in this study had never performed this task before. A training block was conducted to familiarize the subjects with the tracking speed and the cross overlap and to make them comfortable in the working space. In this training block, each of the subjects was allowed to perform 3 arbitrary trials.

3) TESTING BLOCK

During the experiment, each subject conducted a total of 9 trials with each trajectory-dimension condition repeated 3 times (Fig. 2a). The trajectory-dimension conditions were arranged randomly, except that they avoided two successive 3D tracking trials to prevent fatigue.

D. DATA ANALYSIS

1) DATA SELECTION

All data analyses were performed off-line using custom written programs in MATLAB (version R2014a). For the 1D

condition, the kinematic data of the central 800 points of the horizontal line were extracted from the raw data to avoid the turning points, and three such segments were selected from each trial. Two of the segments were in the moving direction from left to right, whereas the other was from right to left. For the 2D and 3D conditions, the second loop of the circular and the cylindrical helical tracking trajectories were selected from the raw data of one trial (Fig. 2b). Therefore, a total of 9 horizontal liner segments, 3 circular loops and 3 cylindrical helical loops from the tracking trajectories in the 1D, 2D and 3D conditions, respectively, were extracted for a single subject since each condition was repeated 3 times. Each measure calculated for each subject was obtained by averaging the results across the 9 segments for the 1D condition, the 3 circular loops for the 2D condition and the 3 cylindrical helical loops for the 3D condition.

2) DATA FILTERING

To calculate RMSE, speed_{sd} and IVPS, the selected data were filtered using a Parks-McClellan lowpass filter with a cut-off frequency of 10 Hz [3]. Since higher order time derivatives were used to calculate Jerk_{m}, a Parks-McClellan bandpass filter between 3 and 11 Hz was used to filter the selected data [28].

3) CALCULATION OF RMSE

The RMSE was calculated as

$$\text{RMSE} = \sqrt{\sum_{i=1}^{N} \frac{[(x_{act}(i) - x_{tar}(i))^2 + (y_{act}(i) - y_{tar}(i))^2}{N}} \times \sqrt{\frac{+(z_{act}(i) - z_{tar}(i))^2]}{N}} \quad (1)$$

where x_{act}, y_{act} and z_{act} represent the 3D spatial coordinates of the actual hand; x_{tar}, y_{tar} and z_{tar} are the coordinates of the target; i denotes the i-th sample; N is the total number of filtered segmental data points.

4) CALCULATION OF SPEED_{sd}

Speed_{sd} is the standard deviation of the magnitude of the speed signals around the mean speed and has been used to describe the speed fluctuations in human movements [2]. It was calculated as follows

$$speed\ (i) = \frac{\sqrt{(x_{act}\ (i+1) - x_{act}\ (i))^2 +}}{\Delta t} \times \frac{\sqrt{(y_{act}\ (i+1) - y_{act}\ (i))^2 + (z_{act}\ (i+1) - z_{act}\ (i))^2}]}{\Delta t} \quad (2)$$

$$\text{speed}_{mean} = \frac{1}{N}\sum_{i=1}^{N} speed(i) \quad (3)$$

$$\text{speed}_{sd} = \sqrt{\frac{1}{N-1}\sum_{i=1}^{N}\left(speed(i) - speed_{mean}\right)^2} \quad (4)$$

where Δt is the time interval of the two consecutive points, and $speed(i)$ denotes the i-th speed sample of the actual hand.

5) CALCULATION OF JERK_m

Jerk_{m} is an index used to measure the 'smoothness' of a signal based on the time derivative of the acceleration, i.e., the third-order derivative of the position [28]. Here, Jerk_{m} was used to reflect the kinematical organization of the 3D submovements. In the 3D spatial version, the square root of the magnitude of the jerk was calculated as

$$\text{Jerk}_m = \sqrt{\frac{\int_{t_{start}}^{t_{end}} \left[\left(\frac{d^3 x_{act}}{dt^3}\right)^2 + \left(\frac{d^3 y_{act}}{dt^3}\right)^2 + \left(\frac{d^3 z_{act}}{dt^3}\right)^2\right] dt}{duration}} \quad (5)$$

where t_{start} and t_{end} indicate the starting and ending time points, respectively; and $duration$ is the interval time between t_{start} and t_{end}.

6) CALCULATION OF IVPS

To ensure the comparability among different conditions, we selected the segmental length of each speed signal when calculating the speed power spectrum over 800 points (Fig. 2b). In the 2D and 3D conditions, the speed signals extracted from the second loop were divided into 4 consecutive segments, each with 800 points. To calculate the IVPS, the selected speed signal was demeaned, and the speed power spectrum was obtained using a fast Fourier transform (800 points padded with zeros to 1024). The resulting 3 speed power spectra for each trial under the 1D condition and 4 speed power spectra for each trial under the 2D and 3D conditions were then averaged separately. Then, we calculated the IVPS in the frequency band of 0.5-1.8 Hz of the averaged speed power spectrum according to Miall *et al*. [20], as follows

$$\text{IVPS} = \sum_{i=5}^{18} p_i \quad (6)$$

where p_i refers to the i-th discrete power density spectrum value. Here, the region of the power spectrum between 0.5 and 1.8 Hz was calculated by summing the power density spectrum values from the 5th to the 18th point since the frequency bin width of the power spectrum was $100/1024 \approx 0.1$ Hz.

7) CALCULATION OF fApEn_{3D}

$\text{fApEn}_{3\text{D}}$ is a 3D version of fApEn, which is an improved approximate entropy (ApEn). fApEn has been used to characterize the nonlinear complexity of short 1D physiological signals [5]. In this paper, we generalized fApEn to its 3D version as follows:

Step 1: Given an N-sample time series with each sample having 3 coordinates $\{x_{act}(i); y_{act}(i); z_{act}(i) : 1 \le i \le N\}$, we separately constructed three vector sequences $\{X_i^m, i = 1, \ldots, N\text{-}m + 1\}$, $\{Y_i^m, i = 1, \ldots, N\text{-}m + 1\}$ and $\{Z_i^m, i = 1, \ldots, N\text{-}m+1\}$ in the m-dimensional space, and all the vector elements in the sequences were subtracted with the averages as

$$\begin{aligned} X_i^m &= \{x_{act}(i), \ldots, x_{act}(i+m-1)\} - \frac{1}{m}\sum_{j=0}^{m-1} x_{act}(i+j) \\ Y_i^m &= \{y_{act}(i), \ldots, y_{act}(i+m-1)\} - \frac{1}{m}\sum_{j=0}^{m-1} y_{act}(i+j) \\ Z_i^m &= \{z_{act}(i), \ldots, z_{act}(i+m-1)\} - \frac{1}{m}\sum_{j=0}^{m-1} z_{act}(i+j) \end{aligned} \tag{7}$$

Step 2: The matrix sequences $\{[X_i^m, Y_i^m, Z_i^m]\}$ were formed by integrating the three vector sequences X_i^m, Y_i^m and Z_i^m. The distance between two adjacent constructed time-series matrices was calculated by the infinite norm

$$\begin{aligned} d_{ij}^m &= \left\| \left[X_i^m, Y_i^m, Z_i^m\right] - \left[X_j^m, Y_j^m, Z_j^m\right] \right\|_\infty \\ &= \left\| \left(X_i^m - X_j^m\right) + \left(Y_i^m - Y_j^m\right) + \left(Z_i^m - Z_j^m\right) \right\|_\infty \end{aligned} \tag{8}$$

where $i \neq j$.

Step 3: The fuzzy similarity degree D_{ij}^m was calculated using a fuzzy function, i.e., an exponential function, as

$$D_{ij}^m(n, r) = \exp\left(-\left(\frac{d_{ij}^m}{r}\right)^n\right) \tag{9}$$

where n and r are the gradient and the width of the boundary of the exponential function. Large n and r values lead to a large gradient and width of the boundary. Moreover, a value of d_{ij}^m closer to unity, results in a higher similarity degree D_{ij}^m.

Step 4: The probability function φ^m averaged all the similarities from any matrices in the time series to another and is expressed as

$$\varphi^m(N, n, r) = \frac{1}{N-m+1} \times \sum_{i=1}^{N-m+1} \ln\left(\frac{1}{N-m+1}\sum_{j=1, j\neq i}^{N-m+1} D_{ij}^m\right) \tag{10}$$

Step 5: Similarly, we obtained the $m + 1$-dimensional constructed matrix sequences $\{\left[X_i^{m+1}, Y_i^{m+1}, Z_i^{m+1}\right]\}$ and the probability function φ^{m+1}. Then, the 3D fuzzy entropy measure $\mathrm{fApEn}_{3D}(m, N, n, r)$ could be estimated as a deviation of the probability function from φ^m to φ^{m+1}

$$\mathrm{fApEn}_{3D}(m, N, n, r) = \varphi^m(N, n, r) - \varphi^{m+1}(N, n, r) \tag{11}$$

where fApEn_{3D} is used to assess the incremental comparisons between the m-and the $m + 1$-dimensional space.

The 4 parameters m, n, r, and N should be defined before each calculation of fApEn_{3D}. Typically [3], [5], [10], the length of the sequence m was typically set to 2 or 3 because a larger m allowed a more detailed reconstruction of the dynamic process, but a too large m value was hard to achieve for a physical dataset or required a very broad boundary, which would lead to information loss [5]. Here, m was selected as 2. Additionally, n and r determined the fuzzy similarity boundary. If the boundary are too narrow, then the fApEn_{3D} would be heavily affected by noise, whereas a too wide boundary might lead to information loss. The fApEn_{3D} had the property of consistency when $N > 300$ and r ranged from 0.02 to 1 using physiological signals [3], [29]. Considering the selected data points for the 1D, 2D and 3D conditions in this study, n, r and N were consequently set to 2, 0.1 and 400, respectively, in this study.

E. STATISTICAL ANALYSIS

All of the parameters are described using the mean ± standard deviation (SD). A one-way repeated-measures analysis of variance (ANOVA) with Bonferroni *post hoc* comparisons was used to analyze the influence of the trajectory dimension on the 5 calculated measures. In addition, a Pearson product-moment coefficient of correlation was utilized to statistically analyze the relationship between each pair of kinematic parameters across the 1D, 2D and 3D conditions. All of the statistical analyses used $p = 0.05$ as the minimal significance level and were conducted using SPSS 19 (SPSS Inc., Chicago, Illinois, USA).

III. RESULT

A. THE ROOT MEAN SQUARE ERROR (RMSE)

The RMSE (Fig. 3a) quantified the tracking accuracy between the actual and target positions. Tests of one-way repeated-measures ANOVA showed that RMSE was significantly influenced by trajectory dimension, and RMSE increased monotonically from 1D to 3D (1D vs. 2D: $p < 0.01$; 2D vs. 3D: $p < 0.01$; 1D vs. 3D: $p < 0.01$).

B. THE STANDARD DEVIATION OF SPEED (SPEED_{sd})

Fig. 2b shows a sample of the 800-point extracted speed signals for the 1D, 2D and 3D conditions, and the mean speeds of these samples are also shown. The mean speeds for different trajectory-dimension conditions were near the target speed (2.25 cm/s), and there were no significant differences between different conditions (1D vs. 2D:$p = 0.725$; 1D vs. 3D: p =0.36; 2D vs. 3D: $p = 0.635$).

The speed signals consisted of speed pulses around their mean values (Fig. 2c). The speed pulses were considered to be related to the submovements of arm tracking, which were segmented small movements due to intermittency. The magnitude of the submovement could be quantified by speed_{sd} to some extent, and speed_{sd} (Fig. 3b) was significantly affected by the trajectory dimension ($p < 0.01$). *Post hoc* comparisons indicated that speed_{sd} significantly increased as trajectory

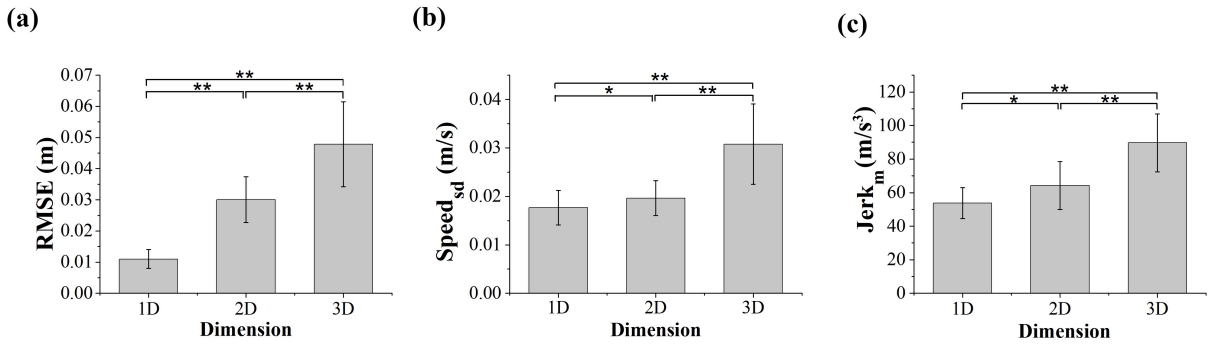

FIGURE 3. Time-domain kinematic measures obtained from the 3 trajectory-dimension conditions. (a) The root mean square error (RMSE). (b) The standard deviation of the speed (speed$_{sd}$). (c) The magnitudinal components of the jerk (Jerk$_m$). Asterisks denote $p < 0.05$, and double asterisks denote $p < 0.01$.

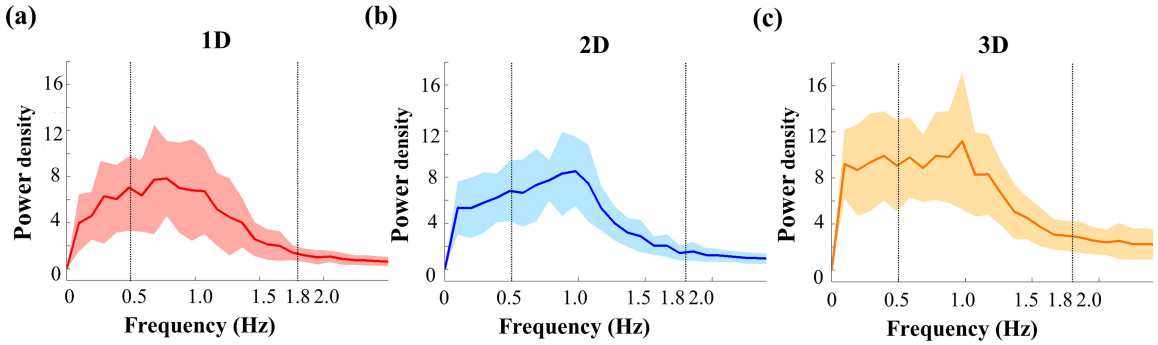

FIGURE 4. The average speed power spectra (solid lines) of the 21 subjects while tracking (a) the straight line (red), (b) the circle (blue) and (c) the cylindrical helix (green) with full visual feedback through an HMD. The shaded regions represent ±1 SD of the mean values. The black vertical dotted lines represent 0.5 Hz and 1.8 Hz.

dimension increased (1D vs. 2D: $p < 0.05$; 1D vs. 3D: $p < 0.01$; 2D vs. 3D: $p < 0.01$).

C. THE MAGNITUDE OF THE JERK (Jerk$_m$)

Fig.3c reveals that the average Jerk$_m$ in the three tracking trajectory dimensions was in the following order: 1D < 2D < 3D ($p < 0.01$). A corresponding Bonferroni *post hoc* test suggested that Jerk$_m$ in each of these conditions was different from the others (1D vs. 2D:$p < 0.05$; 1D vs. 3D: $p < 0.01$; 2D vs. 3D: $p < 0.01$).

D. THE INTEGRAL OF THE SPEED POWER SPECTRUM (IVPS)

Fig. 4 shows the average speed power spectra shaded with ±1 SDs from all 21 subjects under 3 trajectory-dimension tracking conditions with full visual feedback through an HMD.

We calculated the IVPS under different trajectory-dimension conditions within 0.5-1.8 Hz, and the results are shown in Fig. 5. One-way ANOVA with repeated measures showed that the trajectory dimension played a significant role in IVPS ($p < 0.01$). The results of the Bonferroni *post hoc* test showed that a significant difference was found between the 1D and 3D conditions and between the 2D and 3D conditions, but there was no significant difference between the 1D and 2D tasks (1D vs. 3D: $p < 0.01$; 2D vs. 3D: $p < 0.01$).

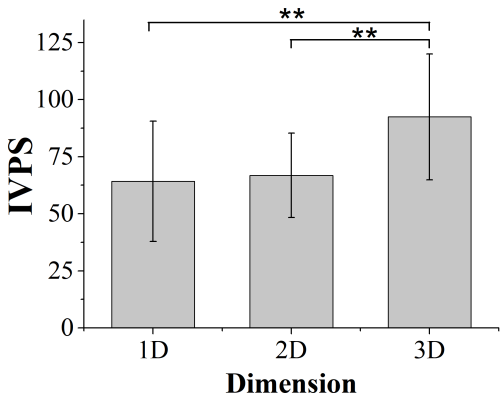

FIGURE 5. The integral of the speed power spectral (IVPS) values in the frequency band of 0.5-1.8 Hz for the 3 different trajectory-dimensional conditions. Asterisks denote $p < 0.05$, and double asterisks denote $p < 0.01$.

E. THE 3D FUZZY APPROXIMATE ENTROPY (fApEn$_{3D}$)

Fig.6 illustrates a notable increase in the mean fApEn$_{3D}$ value of the output trajectories as the trajectory dimension

TABLE 1. The correlations between each pair of kinematic parameters in the 1D, 2D and 3D conditions.

	1D					2D					3D				
	RMSE	$speed_{sd}$	$Jerk_m$	IVPS	$fApEn_{3D}$	RMSE	$speed_{sd}$	$Jerk_m$	IVPS	$fApEn_{3D}$	RMSE	$speed_{sd}$	$Jerk_m$	IVPS	$fApEn_{3D}$
RMSE	1.000					1.000					1.000				
$speed_{sd}$	0.532*	1.000				0.049	1.000				-0.063	1.000			
$Jerk_m$	0.270	0.684**	1.000			0.205	-0.324	1.000			0.109	-0.195	1.000		
IVPS	-0.442*	-0.515*	-0.321	1.000		0.063	0.415	-0.127	1.000		0.101	0.103	-0.505*	1.000	
$fApEn_{3D}$	0.308	0.340	0.115	-0.208	1.000	0.228	-0.106	0.494*	-0.263	1.000	-0.093	0.188	0.012	0.129	1.000

* Correlation was significant at the 0.05 level (2-tailed).
** Correlation was significant at the 0.01 level (2-tailed).

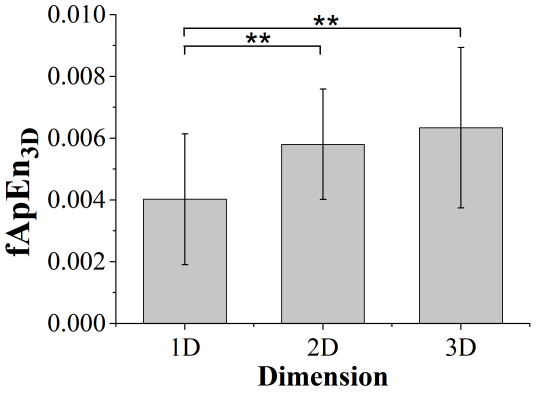

FIGURE 6. The three-dimensional fuzzy approximate entropy ($fApEn_{3D}$) of the actual trajectories. Asterisks denote $p < 0.05$, and double asterisks denote $p < 0.01$.

increased. We used *post hoc* comparisons to examine the dimensionality effect among these three tracking dimensions. The results showed that there was no significant difference between the 2D and 3D conditions ($p > 0.05$), while the differences between the 1D and 2D tasks and between the 1D and 3D conditions were significant (1D vs. 2D:$p < 0.01$; 1D vs. 3D: $p < 0.01$).

F. CORRELATIONAL ANALYSIS

Correlations between each pair of kinematic parameters under different trajectory dimensions are shown in Table 1. For the 1D condition, significant correlations were found between RMSE and $speed_{sd}$ ($p < 0.05$), RMSE and IVPS ($p < 0.05$), $speed_{sd}$ and $Jerk_m$ ($p < 0.01$) and $speed_{sd}$and IVPS ($p < 0.05$) in the 1D condition, while the only significant correlation was between $Jerk_m$ and $fApEn_{3D}$ ($p < 0.05$) in the 2D condition and $Jerk_m$ and IVPS ($p < 0.05$) in the 3D condition.

IV. DISCUSSION

In this study, we built a 3D immersive VE that allowed subjects to follow a moving target with their hands, and we studied the trajectory dimension's effect on sensorimotor control using five kinematic parameters: RMSE, $speed_{sd}$, $Jerk_m$, IVPS and $fApEn_{3D}$.

A. EFFECT OF THE TRAJECTORY DIMENSION ON SENSORIMOTOR CONTROL

The RMSE is a parameter that measures the tracking accuracy and precision of movement. The significantly increased RMSE values in the higher trajectory dimensions in our experiment (Fig. 3a)showed a significant performance deterioration in accuracy in the 2D and 3D conditions. This result is in agreement with that of Watson and Jones [31] and not with Oytam *et al*. [24]. The discrepancies might be accounted for by differences in the experimental design. First, the 1D tracking responses in Oytam *et al*.'s study (2005) were generated by a joystick controlled with the right hand, while the 2D responses were driven by two joysticks controlled bimanually. However, we designed an arm tracking task requiring the distal part of the arm to follow a target cube moving in the 3D VE. As the trajectory dimension increased, the range of joint motion also increased, which led to different collaborative flexions of the elbow and shoulder. The second notable difference was the tracking trajectories. Previous studies [24], [31] examined the trajectory dimension's effect using single and dual-axis tracking tasks, but a curved path was considered to provide more details to reveal the sensorimotor control mechanism [18]. We designed curvilinear tracking trajectories in the 2D condition, beyond which we added a third dimension to the curvilinear trajectory in the 3D condition. 3D visually guided arm tracking is difficult to implement without 3D virtual reality, and the HMD we used in this experiment provided us an effective tool to investigate the trajectory dimension's effect on sensorimotor control. Our results suggest that the deteriorated tracking accuracy in the higher-dimensional conditions might have been due to the much larger range of arm movement.

The $speed_{sd}$ significantly increased as the trajectory dimension increased (Fig. 3b) while the $speed_{mean}$ was not affected by the dimension. Since the multipeaked speed profiles were manifestations of the discrete submovements during arm tracking tasks, the increase in the $speed_{sd}$ value

in the higher trajectory dimension suggests an increase in the amplitude of the submovement. The submovements were considered to correspond to the intermittent error-correction sensorimotor feedback control processes [20] and were not fixed in time or space but instead showed a high correlation with the specific direction and speed error signals [27]. To correct the directional error, the sensorimotor control system aligned the direction of an upcoming submovement at a specific target direction, and a 'slow down - change direction - speed up' movement pattern in the error-corrective process was present but has an energy cost [3]. The larger $speed_{sd}$ in the 2D and 3D conditions might have been due to more movement directions predetermined by the target trajectory, and a larger speed fluctuation and a relatively larger amplitude of the error-corrected submovements suggests an increase in the energy cost.

The time-domain jerk parameter ($Jerk_m$) has been widely used to measure the smoothness of the movement trajectory [28] and the coordination of multijoint human movement [10]. In this study, significantly higher $Jerk_m$ values were found in the higher trajectory dimensions (Fig. 3c), which demonstrates that movements made by subjects became less smooth, and the multiple joints were less coordinated. Recent studies have revealed that increasing both the target distance [34] and movement direction [11] influences the coordinated movement response. Other studies have illustrated that to achieve necessary positions, the sensorimotor system should regulate sequential muscle control for the subsequent coordination [6], [15]. Compared with the 1D task, subjects coordinated their shoulder and elbow joints to make the distal part of the arm follow the target in a larger space with more movement directions. Therefore, tracking a trajectory with a higher dimension increased the demand for the coordination of multijoint human movements.

In this experiment, the higher IVPS value in the 3D condition compared with the lower-dimensional conditions (Fig. 5) implied that increasing the trajectory dimension led to a significant increase in the signal power of tracking responses between 0.5 and 1.8 Hz. According to Miall *et al*. [20], the power in the frequency band of 0.5-1.8 Hz during tracking with visual feedback is larger than that without visual feedback, which reflected the intermittency in tracking behaviors when subjects used visual information as tracking-error feedback. The higher IVPS values in the higher-trajectory-dimension conditions in our experiment might have been due to the larger magnitude of the error-corrective submovements during the visuomotor feedback control loop. Furthermore, motor behaviors reflect a combination of feedforward and feedback control by the human CNS [1], [35]. Feedforward control is driven by the internal model [32], while feedback control refers to a modification of movement due to sensory information that involves error detection and error correction [7], [35]. The responding trajectory in the 1D condition might have been a result of the short-term prediction of target motion according to the internal model since the subject was relatively more familiar with the linear tracking tasks [19], [22], [23]. Our results suggest the visual information dependency of arm tracking and a shift to heavier feedback control as trajectory dimension increases.

Entropy has been used as a measure of complexity and regularity in nonlinear systems [25]. An advantage of the entropy-based approach is that it encompasses the capability of adjusting movement behaviors customized for the tasks and environmental contexts [10]. As a nonlinear measure, $fApEn_{3D}$ might capture the nonlinear nature of the sensory and motor systems [9], [33], e.g., multiple inputs and unknown error deadzones [26]. As a measure of complexity, $fApEn_{3D}$ reflected the level of neuromotor noise during sensorimotor control [7], [19]. In our experiment, the increase of $fApEn_{3D}$ in the higher dimensional conditions might have been due to a greater amount of sensory input information, i.e., more moving directions in the 2D and 3D conditions [3], [30]. In addition, the signal-dependent neuromotor noise in the motor system would increase in the 2D and 3D conditions with a larger movement space [8], [19]. We speculated that the higher neuromotor noise level might be related to the higher $fApEn_{3D}$ values in the 2D and 3D conditions.

B. CORRELATIONS BETWEEN EACH PAIR OF KINEMATIC PARAMETERS

This study used multiple kinematic parameters to investigate the dimension-induced trajectory changes in sensorimotor control during arm tracking tasks. Correlational analysis between each pair of kinematic parameters in the order trajectory-dimension condition is shown in Table 1. In the 1D condition, 4 significant correlations (RMSE and $speed_{sd}$, RMSE and IVPS, $speed_{sd}$ and $Jerk_m$, $speed_{sd}$ and IVPS) were found, which is consistent with the results of Miall *et al*. [20]. High correlations indicate the consistency of RMSE, $speed_{sd}$, $Jerk_m$ and IVPS parameters and revealed their worth in the kinematic evaluation of the 1D condition. However, moderate correlations with almost all the kinematic parameters were demonstrated in the 2D and 3D conditions. This result might be because the kinematic parameters had higher responsiveness and were more sensitive to movement directions [27]. We speculate that in the 1D condition, the manner in which subjects performed the horizontal straight linear tracking task with a fixed direction was less influenced by direction, while subjects needed to regulate not only movement speed but also movement direction in real time in the 2D and 3D conditions.

In general, relatively high correlations were found in the 1D condition, and moderate correlations were found in the 2D and 3D conditions. We suspect that the kinematic parameters selected in this study made different contributions to investigating the trajectory dimension-induced changes in sensorimotor control. The only error signals [31] might be limited for complex human movements, so it was necessary to use multiple kinematic parameters (i.e., time- and frequency-domain measures, linear and nonlinear measures) to create an effective and comprehensive set of outcome measures of

trajectory dimension-induced changes in sensorimotor control during arm tracking tasks.

C. FUTURE WORK AND POTENTIAL APPLICATIONS

The limitation of this work is as follows: first, diseases might influence different stages of the sensorimotor control, but we recruited only healthy youths; second, in this study, we only recorded kinematic data. In the future, we could recruit patients with CNS disease which related to motor problems. In addition, other physiological signals such as electromyography (EMG), functional near-infrared spectroscopy (fNIRS), or electroencephalography (EEG) could be recorded combined with kinematic data during 3D arm tracking to investigate the sensorimotor control mechanisms from other aspects.

The experimental paradigms can be used as a tool in the clinical evaluation of disabled persons. These free upper limb tracking tasks performed in 3D space closely resemble daily activities and can be applied to purposeful interventions in physical rehabilitation to maximize and maintain the effectiveness of rehabilitation. Additionally, the multijoint arm movement proposed in this study can serve as a guideline to determine other external factors, such as the range of joint motion, target speeds and target sizes, within which the examination setup can be well controlled since virtual reality has the ability to provide a standardized, reproducible and controllable environment.

V. CONCLUSION

This study built a 3D immersive VE that allowed subjects to follow a moving target with their hands, and we studied the trajectory-dimension effect on sensorimotor control. We used multiple kinematic parameters, including time-domain (RMSE, speed_{sd} and Jerk_{m}) and frequency-domain properties (IVPS), as well as linear (RMSE, speed_{sd}, Jerk_{m} and IVPS) and nonlinear measures ($\text{fApEn}_{3\text{D}}$). Correlations between each pair of kinematic parameters showed that the multiple kinematic measures could provide a comprehensive perspective of sensorimotor control during arm tracking tasks, especially in the higher trajectory dimensional conditions.

ACKNOWLEDGMENT

The authors would like to thank all the participants and Haizhen Luo and Yongkeng Fan for doing parts of the experiments and data collection.

REFERENCES

[1] D. Ao, R. Song, and K.-Y. Tong, "Sensorimotor control of tracking movements at various speeds for stroke patients as well as age-matched and young healthy subjects," *PLoS ONE*, vol. 10, no. 6, p. e0128328, Jun. 2015.

[2] T. M. Barbosa, K. L. Keskinen, R. Fernandes, P. Colaço, A. B. Lima, and J. P. Vilas-Boas, "Energy cost and intracyclic variation of the velocity of the centre of mass in butterfly stroke," *Eur. J. Appl. Physiol.*, vol. 93, nos. 5–6, pp. 519–523, Mar. 2005.

[3] T. M. Barbosa, W. X. Goh, J. E. Morais, M. J. Costa, and D. Pendergast, "Comparison of classical kinematics, entropy, and fractal properties as measures of complexity of the motor system in swimming," *Frontiers Psychol.*, vol. 7, p. 1566, Sep. 2016.

[4] Z. Cao *et al.* (Sep. 2018). "Extraction of SSVEPs-based inherent fuzzy entropy using a wearable headband EEG in migraine patients." [Online]. Available: https://arxiv.org/abs/1809.06673

[5] W. Chen, Z. Wang, H. Xie, and W. Yu, "Characterization of surface EMG signal based on fuzzy entropy," *IEEE Trans. Neural Syst. Rehabil. Eng.*, vol. 15, no. 2, pp. 266–272, Jun. 2007.

[6] A. Choi, S. B. Joo, E. Oh, and J. H. Mun, "Kinematic evaluation of movement smoothness in golf: Relationship between the normalized jerk cost of body joints and the clubhead," *Biomed. Eng. OnLine*, vol. 13, no. 20, p. 20, Feb. 2014.

[7] D. W. Franklin and D. M. Wolpert, "Computational mechanisms of sensorimotor control," *Neuron*, vol. 72, no. 3, pp. 425–442, Nov. 2011.

[8] C. M. Harris and D. M. Wolpert, "Signal-dependent noise determines motor planning," *Nature*, vol. 394, no. 6695, pp. 780–784, Aug. 1998.

[9] N. Hogan and D. Sternad, "Sensitivity of smoothness measures to movement duration, amplitude, and arrests," *J. Motor Behav.*, vol. 41, no. 6, pp. 529–534, Nov. 2009.

[10] S. Lee Hong and K. M. Newell, "Entropy compensation in human motor adaptation," *Chaos, Interdiscipl. J. Nonlinear Sci.*, vol. 18, no. 1, pp. 1299–1313, Apr. 2008.

[11] Y. Huang, Q. Yang, Y. Chen, and R. Song, "Assessment of motor control during three-dimensional movements tracking with position-varying gravity compensation," *Frontiers Neurosci.*, vol. 11, p. 253, May 2017.

[12] A. M. Hughes, C. T. Freeman, J. H. Burridge, P. H. Chappell, P. L. Lewin, and E. Rogers, "Shoulder and elbow muscle activity during fully supported trajectory tracking in people who have had a stroke," *J. Electromyogr. Kinesiol.*, vol. 20, no. 3, pp. 465–476, Jun. 2010.

[13] M. A. Huysmans, M. J. M. Hoozemans, A. J. van der Beek, M. P. de Looze, and J. H. van Dieën, "Submovement organization, pen pressure, and muscle activity are modulated to precision demands in 2D tracking," *J. Motor Behav.*, vol. 44, no. 5, pp. 379–388, Sep. 2012.

[14] Y. H. Kee, N. N. L. D. Chatzisarantis, P. W. Kong, J. Y. Chow, and L. H. Chen, "Mindfulness, movement control, and attentional focus strategies: Effects of mindfulness on a postural balance task," *J. Sport Exercise Psychol.*, vol. 34, no. 5, pp. 561–579, May 2012.

[15] J. Laczko, R. A. Scheidt, L. S. Simo, and D. Piovesan, "Inter-joint coordination deficits revealed in the decomposition of endpoint jerk during goal-directed arm movement after stroke," *IEEE Trans. Neural Syst. Rehabil. Eng.*, vol. 25, no. 7, pp. 798–810, Jul. 2017.

[16] L. Liang, Z. Yang, M. Zhang, and Y. Pan, "Revealing the radial effect on orientation discrimination by manual reaction time," *Frontiers Neurosci.*, vol. 11, p. 638, Nov. 2017.

[17] J. Limanowski, E. Kirilina, and F. Blankenburg, "Neuronal correlates of continuous manual tracking under varying visual movement feedback in a virtual reality environment," *Neuroimage*, vol. 146, pp. 81–89, Feb. 2017.

[18] L. Liu and R. Van Liere, "Modeling object pursuit for desktop virtual reality," *IEEE Trans. Vis. Comput. Graphics*, vol. 18, no. 7, pp. 1017–1026, Jul. 2012.

[19] P. H. McCrea and J. J. Eng, "Consequences of increased neuromotor noise for reaching movements in persons with stroke," *Exp. Brain Res.*, vol. 162, no. 1, pp. 70–77, Mar. 2005.

[20] R. C. Miall, D. J. Weir, and J. F. Stein, "Intermittency in human manual tracking task," *J. Motor Behav.*, vol. 25, no. 1, pp. 53–63, Apr. 1993.

[21] L. A. Mrotek, C. C. A. M. Gielen, and M. Flanders, "Manual tracking in three dimensions," *Exp. Brain Res.*, vol. 171, no. 1, pp. 99–115, 2006.

[22] P. D. Neilson, M. D. Neilson, and N. J. O'Dwyer, "Internal models and intermittency: A theoretical account of human tracking behavior," *Biological*, vol. 58, no. 2, pp. 101–112, Feb. 1988.

[23] P. D. Neilson and M. D. Neilson, "An overview of adaptive model theory: Solving the problems of redundancy, resources, and nonlinear interactions in human movement control," *J. Neural Eng.*, vol. 2, no. 3, pp. S279–S312, Jul. 2005.

[24] Y. Oytam, P. D. Neilson, and N. J. O'Dwyer, "Degrees of freedom and motor planning in purposive movement," *Hum. Movement Sci.*, vol. 24, nos. 5–6, pp. 710–730, 2005.

[25] S. Pincus, "Approximate entropy (ApEn) as a complexity measure," *Chaos, Interdiscipl. J. Nonlinear Sci.*, vol. 5, no. 1, pp. 110–117, 1995.

[26] J. H. Pérez-Cruz, J. D. J. Rubio, E. Ruiz-Velázquez, and G. Solís-Perales, "Tracking control based on recurrent neural networks for nonlinear systems with multiple inputs and unknown deadzone," *Abstract Appl. Anal.*, vol. 2012, pp. 1–18, 2012, Art. no. 471281. [Online]. Available: https://www.hindawi.com/journals/aaa/2012/471281/

[27] A. V. Roitman, S. G. Massaquoi, K. Takahashi, and T. J. Ebner, "Kinematic analysis of manual tracking in monkeys: Characterization of movement intermittencies during a circular tracking task," *J. Neurophysiol.*, vol. 91, no. 2, pp. 901–911, 2004.
[28] K. Schneider and R. F. Zernicke, "Jerk-cost modulations during the practice of rapid arm movements," *Biological*, vol. 60, no. 3, pp. 221–230, 1989.
[29] W. Sun, J. Liang, Y. Yang, Y. Wu, T. Yan, and R. Song, "Investigating aging-related changes in the coordination of agonist and antagonist muscles using fuzzy entropy and mutual information," *Entropy*, vol. 18, no. 6, p. 229, Jun. 2016.
[30] N. Thibbotuwawa, R. S. Goonetilleke, and E. R. Hoffmann, "Constrained path tracking at varying angles in a mouse tracking task," *Hum. Factors, J. Hum. Factors Ergonom. Soc.*, vol. 54, no. 1, pp. 138–150, Feb. 2012.
[31] R. W. Watson and R. D. Jones, "A comparison of two-dimensional and one-dimensional tracking performance in normal subjects," *J. Motor Behav.*, vol. 30, no. 4, pp. 359–366, Dec. 1998.
[32] D. M. Wolpert and M. Kawato, "Multiple paired forward and inverse models for motor control," in *Proc. Conf. Adv. Neural Inf. Process. Syst.*, vol. 11, 1999, pp. 31–37.
[33] C. Yang, A. Kerr, V. Stankovic, L. Stankovic, P. Rowe, and S. Cheng, "Human upper limb motion analysis for post-stroke impairment assessment using video analytics," *IEEE Access*, vol. 4, pp. 650–659, 2016.
[34] Q. Yang, Y. Yang, J. Luo, L. Li, T. Yan, and R. Song, "Kinematic outcome measures using target-reaching arm movement in stroke," *Ann. Biomed. Eng.*, vol. 45, no. 12, pp. 2794–2803, Dec. 2017.
[35] S.-H. Yeo, D. W. Franklin, and D. M. Wolpert, "When optimal feedback control is not enough: Feedforward strategies are required for optimal control with active sensing," *PLoS Comput. Biol.*, vol. 12, no. 2, p. e1005190, Feb. 2016.

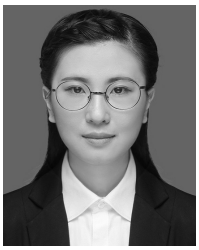

MENGYING FAN was born in Huzhou, Zhejiang, China, in 1993. She is currently pursuing the master's degree with Sun Yat-sen University, Guangzhou, China.

JIE LUO received the B.S., M.S., and Ph.D. degrees in biomedical engineering from the Huazhong University of Science and Technology, Wuhan, in 2004, 2007, and 2012, respectively.

Since 2013, she has been a Lecturer with the School of Biomedical Engineering, Sun Yat-sen University. Her current research interest includes the effects of diseases on neuromotor control.

LE LI received the Ph.D. degree from the Department of Health Technology and Informatics, The Hong Kong Polytechnic University, in 2007. He completed the Postdoctoral training at The Hong Kong Polytechnic University, in 2010. From 2014 to 2016, he was a Visiting Scientist with the TIRR Memorial Hermann Research Center and the Department of Physical Medicine and Rehabilitation, UTHealth, Houston, TX, USA. He is currently an Associate Professor with the Department of Rehabilitation Medicine, The First Affiliated Hospital, Sun Yat-sen University, Guangzhou, China. His current research interests include biosignal processing (electromyography), neuromusculoskeletal modeling of normal and spastic subjects, and musculoskeletal ultrasound application.

DONG FENG HUANG was a Visiting Professor with the Rusk Institute of Rehabilitation Medicine, NYU Langone Health, from 2010 to 2011. He is currently a Professor and the Head of the Faculty of Rehabilitation Sciences, Sun Yat-sen University. He is also the Head of the WHO Collaborating Center for Rehabilitation, The First Affiliated Hospital, Sun Yat-sen University, Guangzhou. His current research interests include rehabilitation medicine, neurorehabilitation, and rehabilitation engineering.

YINWEI ZHAN was born in Changchun, Jilin, China, in 1966. He received the B.S. degree in mathematics and the M.S. degree in computational mathematics from Jilin University, in 1986 and 1988, respectively, and the Ph.D. degree in computational mathematics from Dalian University, in 1992. He held a Postdoctoral position with Beijing Normal University, until 1994. From 1994 to 2001, he was an Associate Professor in mathematics with Shantou University. From 2001 to 2004, he held a Postdoctoral position with CWI, Amsterdam, and Groningen University. Since 2005, he has been a Full Professor with the School of Computer, Guangdong University of Technology, where he is leading the Interactive and Visual Informatics Team.

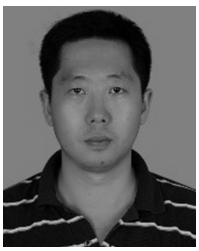

RONG SONG received the B.S. degree in electrical engineering from Tsinghua University, Beijing, China, in 1999, the M.S. degree in electronic engineering from Shantou University, Shantou, China, in 2002, and the Ph.D. degree in biomedical engineering from The Hong Kong Polytechnic University, Hong Kong, in 2006. He is currently a Professor with the School of Biomedical Engineering, Sun Yat-sen University, China. His current research interests include musculoskeletal modeling, biomedical signal processing, human motion analysis, and robot-assisted stroke rehabilitation.